IEEE Access
Multidisciplinary | Rapid Review | Open Access Journal

Received 28 February 2024, accepted 10 March 2024, date of publication 2 April 2024, date of current version 10 April 2024.

Digital Object Identifier 10.1109/ACCESS.2024.3384258

RESEARCH ARTICLE

Automated Method for Uterine Contraction Extraction and Classification of Term Versus Pre-Term EHG Signals

RUBANA HOQUE CHOWDHURY[1], QUAZI DELWAR HOSSAIN[1], (Member, IEEE), AND MOHIUDDIN AHMAD[2], (Member, IEEE)

[1]Department of Electrical and Electronic Engineering, Chittagong University of Engineering and Technology, Chittagong 4349, Bangladesh
[2]Department of Electrical and Electronic Engineering, Khulna University of Engineering and Technology, Khulna 9203, Bangladesh

Corresponding author: Rubana Hoque Chowdhury (rubanachy@gmail.com)

This work involved human subjects or animals in its research. The authors confirm that all human/animal subject research procedures and protocols are exempt from review board approval.

ABSTRACT The significance of uterine contractions in facilitating the successful birth of fetuses is self-evident. Timely recognition of high-risk deliveries, coupled with the administration of appropriate medication, has emerged as a promising approach to address this concern. However, the quest for effective early diagnostic methods continues to present a challenge in the field. The objective of this study was to develop a fully automated methodology for the identification of both normal and premature deliveries using EHG signals. In this study, a freely accessible database was utilized, comprising 338 signals obtained from two distinct groups of pregnant women: those who delivered at term (281 records) and those who experienced preterm delivery (57 records). The methodology employed in this study is structured into three sequential steps. Firstly, contraction segments are extracted utilizing an amplitude modulation technique. Subsequently, a process is implemented to identify consistent contractions by correlating the extracted segments with the tocodynamometer (TOCO) signal. In this step, the consistency index is assessed. Lastly, features such as energy, contraction intensity, contraction duration, peak-to-peak amplitude, log detector, and Shannon entropy are extracted from each contractile activity segment, statistical analysis was conducted using a non-parametric Mann-Whitney U test to identify significant features, and a Random forest (RF) is employed for the classification and discrimination between term and preterm births. The findings of this study show that the average consistency Index (CCI) during pre-term conditions is 0.91, contrasting with a value of 0.9 during term conditions after the extraction of contraction segments. Moreover, our experimental research results display that the performance of RF can achieve an Accuracy of 89%, Sensitivity of 85.87%, and precision of 88.76%. Our results suggest that this simple and effective method can automatically recognize uterine contraction and differentiate between term and preterm EHG signals. This may pave the way for innovative applications in the prevention of preterm labor.

INDEX TERMS EHG, feature extraction, uterine contraction, random forest, zero-crossing rate.

I. INTRODUCTION

Electrohyterogram (EHG) has recently gained popularity as a method for assessing and detecting obstetric-related issues and labor outcomes. EHG monitoring systems have become more prevalent in the research field because of the possible detection of many obstetric problems that are life threatening for pregnant women and their babies. Modern healthcare relies on aggressive treatments with possible side effects, causing anxiety in pregnant women and their

The associate editor coordinating the review of this manuscript and approving it for publication was Kin Fong Lei.

families, neglecting other children, etc. There is a high cost associated with threatened preterm deliveries for medical procedures and the economy as a whole. Therefore, Researchers are persistently concentrating on the use of EHG for long-term UC monitoring and obstetric outcome prediction. L. Pin et al. [1] showed that EHG is useful for clinical diagnosis and labor management since it is a non-invasive, integrative, and quantitative method for evaluating the effectiveness of uterine contractions (UCs). Labor, the physiological procedure through which a fetus is expelled from the uterus, is characterized by regular uterine contractions, cervical effacement, and dilation. The World Health Organization (WHO) defines preterm birth as labor starting earlier than expected and the baby being born before 37 weeks of pregnancy has passed 37–42 weeks as a term, and over 42 weeks as post-term [2]. Experiencing complications during pregnancy can lead to premature birth which consistently increases the risk of the physical condition of very preterm children and parental mental health problems [3], [4]. Uterine contraction (UC) is a vital diagnostic tool for monitoring uterine activity during pregnancy and labor. During pregnancy, UC evaluates the advancement of labor and delivery substantially. Previously researchers had paid big attention to fetal heart rate (FHR) to interpret the cardiotocogram (CTG). However, thorough UC monitoring is just as crucial for determining CTG as FHR [5]. Generally, two techniques external tocodynamometry (TOCO) and Intrauterine Pressure Catheters (IUPC) have been used for monitoring UC. In the TOCO method, a pressure transducer was placed on the patient's abdomen and contractions were measured. The intrauterine pressure significantly changes as a result of the uterine contractions [2]. It detects pressure force produced by the contorting abdomen and converts this mechanical energy to an electrical signal. The strain applied by the uterine muscle through the abdominal wall to the strain gauge transducer results in a straightforward transformation into the TOCO signal. Moreover, it can be affected by subcutaneous fat content and is subject to movement artifacts. The intrauterine pressure catheter (IUPC) directly detects the intrauterine pressure changes brought on by UCs, however, its invasiveness poses a risk of infection and membrane rupture. Researchers have been exploring different techniques and trying to find out safe and accurate alternatives. Recently EHG has been considered a non-invasive technique for UC monitoring which is a specific form of electromyography (EMG). Electrophysiological monitoring of the uterine-muscle activity, referred to as an electrohysterogram, is essential to permit timely treatment during pregnancy. In this technique, electrodes are placed on the abdominal surface of pregnant women which represents the electrical activity of the uterine muscle. In 1950, Steer and Hertsch originally suggested the name electrohysterography (EHG) [6].

Recently, researchers have been continuously trying to extract features from individual contraction intervals or non-contraction intervals using entire EHG signals to predicting pre-term birth [7], [8], [9], [10], [11], [12], [13]. The successful progression of labor and delivery relies on the occurrence of consistent and efficient contractions of the uterine myometrium. The mechanisms governing the onset and continuity of appropriate and coordinated uterine activity crucial for labor and delivery involve an intricate interplay of hormonal, mechanical, and electrical factors. However, these factors have not been comprehensively understood or elucidated yet [14]. This has motivated researchers to dedicate efforts to investigating the contractile segment of electrohysterogram (EHG) signals. From the literature review, it was observed that many studies only focused on uterine contractile activity instead of the full EHG signal because the contraction activity of the EHG signal carries important information. However, the majority of research findings rely on manually annotated EHG uterine contractions, presenting an ongoing challenge [8], [10], [11], [12]. Consequently, the implementation of an algorithm for autonomous contraction identification based on EHG signals is imperative. Additionally, the development of a computational method for the recognition of preterm delivery holds significant importance in facilitating timely diagnosis and treatment of this condition. The contributions of this study were

Extract uterine contraction segment automatically from the entire EHG signal using amplitude modulation technique.

The proposed model automatically detects premature and normal births using the significant features from automatically segmented contractions.

To enhance the clarity of our presentation, the remainder of the paper is structured as follows: Section II provides a comprehensive overview of related work. Section III provides a comprehensive overview of the database used and outlines the methodology step by step, accompanied by relevant figures. Section IV presents the experimental results. Section V delves into the discussion of the findings, identifying areas for further research. Section VI offers concluding remarks, summarizing the primary contributions of this study.

In summary, the suggested algorithm exhibits good accuracy and straightforward computational requirements, rendering it suitable for real-time applications in the detection of premature births and the extended monitoring of uterine contractions.

II. RELATED WORK

In this section, we have delineated four studies specifically focusing on the automatic extraction of uterine contraction bursts from the entire electrohysterogram (EHG) signal.

Esgalhado et al. [15] presented five different energy burst methods, including wavelet energy, Teager energy, root mean square (RMS), squared RMS, and Hilbert envelope for contraction detection. They utilized the Icelandic 16-electrode (4 by 4 grid) EHG database, comprising 122 recordings from 45 pregnant subjects, with only four cases of preterm birth. Their observations indicated that squared RMS yielded the highest contraction accuracy ($97.15 \pm 4.66\%$) and delineation accuracy ($89.43 \pm 8.10\%$), along with the lowest false positive rate (0.63%). However, the study lacks measurement

of the contraction consistency index (CCI) using any existing technique, and there is no verification of the method in any practical application. Furthermore, the study's data size was too small.

Muszynski et al. [16] tested the feasibility and accuracy of uterine contraction detection based on nonlinear correlation coefficient analysis and compared it to an expert decision using external tocodynamometry (TOCO). The study utilized 51 recordings obtained from two distinct groups of pregnant women: laboring mothers and women at risk of preterm birth. These recordings were conducted using a setup comprising 16 electrodes. They used a nonlinear correlation coefficient as a feature for contraction detection, and the reported detection rates were 62.5 % (full detections), and 37.5% (partial detections). A notable limitation of this study is the high false detection rate and the relatively small size of the dataset utilized.

Chen et al. [17] designed an adaptive threshold technique with entropy analysis for detecting contraction onset/offset locations. The study utilized the Icelandic 16-electrode (4 by 4 grid) EHG database as its primary data source. They compared their method with the existing root mean square methods and showed that the contraction detection rate of the proposed method reaches 87.9%. Following the detection of contractions, features (mean frequency, median frequency, and Detrended fluctuation analysis) were extracted and they showed that there were significant differences existed between non-labor and labor categories. However, the study lacks an evaluation of the CCI using any existing technology, and a relatively small dataset was used.

Song et al. [18] employed a combination of zero-crossing rate (ZCR) and root mean square (RMS) techniques to modulate the EHG signal. This approach was utilized to effectively highlight EHG contraction segments within the signal. Using eight-channel electrodes, they made 54 recordings, of which only 4 were preterm deliveries and the remaining 50 were term deliveries. Their findings demonstrated that the electrohysterogram (EHG) had a lower number of falsely recognized uterine contractions (FP) and non-contractions (FN) compared to TOCO, as assessed by maternal perception. The authors reported that the sensitivity and positive predictive value (PPV) based on UCs detection for EHG were 87.8% and 93.18%, respectively, which exceeded those of TOCO. No results were reported on the CCI and a small dataset was used. The proposed system has not been implemented in any practical applications.

The previously proposed systems exhibit limitations including:

- Did not report important evaluation criteria such as the CCI index.
- Do not apply in any application such as predicting premature birth or labor outcome.
- Employment of a redundant number of electrodes.
- Reliance on a small dataset for analysis.

Our proposed system offers improvements over these limitations in the following aspects:

- Reduced utilization of electrodes for uterine contractions detection
- Evaluation of the CCI index using existing technology.
- Utilization of larger datasets for comprehensive analysis and validation.
- Applicable for premature and normal births.

III. MATERIAL AND METHODS

The step-by-step process of EHG data acquisition, EHG signal preprocessing, automatic contraction segmentation, feature extraction, and classification is explained in the following paragraphs. The details of each step of the method are presented in Fig. 1.

A. DATA COLLECTION DESCRIPTION

Nowadays many researchers work on automated detection techniques to process the EHG signal which appears appropriate for outpatient monitoring of uterine contractions [16]. A large EHG signal database will aid in improving techniques for predicting the mode of birth delivery and preterm birth. This makes it vital to collect a lot of EHG signals from pregnant women of various gestational ages. For long-term monitoring of UCs, interference component removal from the measured EHG signals, and real-time analysis of EHG signals, several studies used a variety of electrode configuration protocols on the lower abdomen of pregnant women [18], [20], [21], [22], [23], [24] Franc Jager et al. [7] were acquired EHG signal from 1997 until 2006 at the Department of Obstetrics and Gynecology, Medical Centre Ljubljana, Ljubljana and later in 2018 they again developed a new set of uterine records (EHG signals accompanied by a simultaneously recorded TOCO signal) of pregnant women (preterm, term). The dataset TPEHG DB (without TOCO) contains 300 records (262 term records, and 38 preterm records) and TPEHGT DS (with TOCO) contains 26 three-signal 30-min uterine EHG records (13 preterm records, and 13 term records from eight and ten pregnant women respectively) [7], [24].

In their study, they acquired thirty-minute uterine recordings from the abdominal surface using a 4-electrode (e1, e2, e3, e4) placement protocol which is shown in Fig. 2. Both datasets are freely available on the Physionet website (https://physionet.org/physiobank/database/tpehgt/ and https://physionet.org/physiobank/database/tpehgdb/). In our study, we used a total of 338 uterine EHG signals from these two publicly available uterine contraction EHG signal databases. However, after the preprocessing step, our method split into two steps:

1. The extraction of contraction information from EHG used the tpehgt_TXXX records from the TPEHGT DS database because the evaluation of this method requires a reference signal for comparison. This database provides the TOCO signal with EHG simultaneously and provides the manual contraction interval information in the atr file.

2. The aforementioned approach was then applied to a total of 338 uterine EHG signals to detect premature birth.

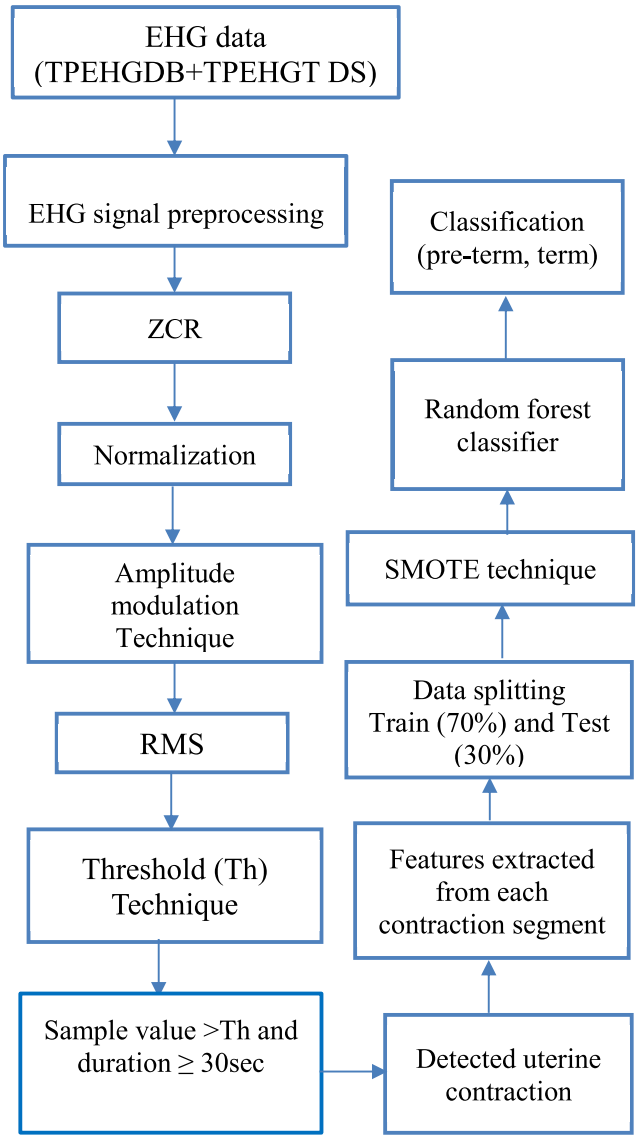

FIGURE 1. Flowchart of the method.

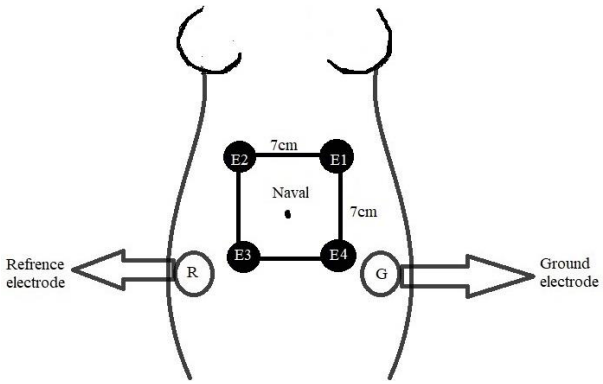

FIGURE 2. Four electrode placements on the lower abdomen spaced seven cm apart.

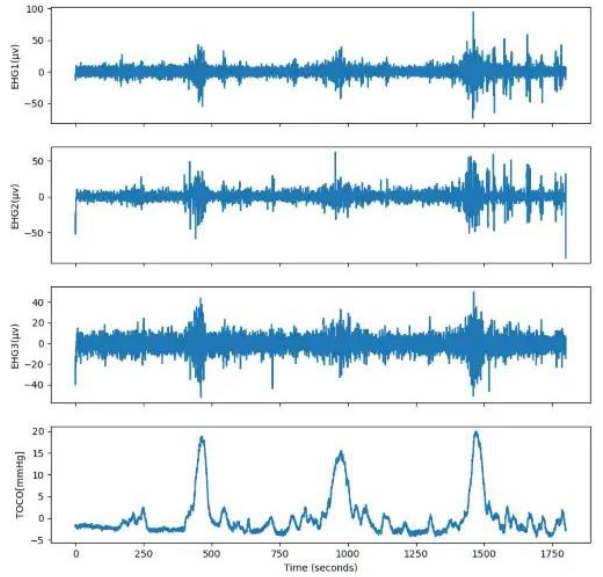

FIGURE 3. Sample of EHG and TOCO signal (record tpehgt_p008). From the top, the first one is the EHG1 signal which was measured by the potential difference the electrode e2 and electrode e1 (EHG1=e2-e1); the second one EHG2 signal was measured between electrode e2 and electrode e3 (EHG2=e2- e3); the third one EHG3 signal was measured between the electrode e4 and the electrode e3 (EHG3=e4-e3). The fourth one is the TOCO signal.

Fig. 3 represents three channel EHG signals, EHG1 (channel 1: e2-e1), EHG2 (channel 2: e2-e3), EHG3 (channel 3: E4-E3), and simultaneously recorded TOCO signal. These signals were sampled at 20 Hz, and the EHG and TOCO signals were bandpass filtered between 0.08 and 5.0 Hz using a 4-pole digital Butterworth filter. Signal EHG1 and EHG3 measure the difference in electric potentials between the top and bottom horizontally positioned electrodes. Signal EHG2, on the other hand, evaluates the differentiation between the left vertically positioned electrodes. Signal EHG3 is likely to have stronger frequency components reflecting the equivalent uterine mechanisms because it is closer to the cervix [7]. A recent study found that the EHG from channel 3 was the most distinct signal for distinguishing preterm and term deliveries [8]. In light of their findings, channel 3 was specifically selected in our study to assess the effectiveness of our technique in identifying uterine contraction segments.

Butterworth filter Signal EHG1 and EHG3 measure the difference in electric potentials between the top and bottom horizontally positioned electrodes. Signal EHG2, on the other hand, evaluates the differentiation between the left vertically positioned electrodes. Signal EHG3 is likely to have stronger frequency components reflecting the equivalent uterine mechanisms because it is closer to the cervix [7]. A recent study found that the EHG from channel 3 was the most distinct signal for distinguishing preterm and term deliveries [8]. In light of their findings, channel 3 was specifically selected in our study to assess the effectiveness of our technique in identifying uterine contraction segments.

B. PREPROCESSING

The databases downloaded from the PhysioNet website are in the WFDB (waveform database) signal files format which is

easily processed in Python by installing the wfdb software package [https://physionet.org/content/wfdb-python/4.1.0/]. The signal obtained from the lower abdomen is a complicated amalgamation of mother electrocardiogram (MECG), foetal electrocardiogram (FECG), and other signals. uterine activity signals (UA), myographic signals, and various other signals [25]. The EHG contains two signals - a slow wave and a fast wave. The slow wave ranges from 0.005 to 0.03 Hz with amplitude between 0.5 mV and 15 mV. The fast wave varies from 0.1 to 3 Hz with amplitude between 0.02 mV and 0.5 mV respectively. In the form of an EHG signal, the fast wave is superimposed on the slow wave. For the purpose of extraction of the signal of uterine activity, EHG signals have been passed through the 4th-order Butterworth filter of 0.01 -3 Hz.

C. RECOGNITION OF CONTRACTION SEGMENT

In the following section, we will thoroughly discuss the systematic extraction process of contraction segments from the EHG signal:

1) ZERO- CROSSING RATE

Zero Crossing rate (ZCR) is characterized by the count of instances in which a (digital) signal crosses zero, serving as an approximation of the signal frequency. In many applications, different authors utilize different approaches to calculate this value [26], [27], [28], [29], [30], [31]. Radhakrihnan first observed that first-order zero crossing rates differentiate contraction and non-contraction segments efficiently using TOCO [32]. In this study, we used a zero-crossing rate from the EHG3 signal as per the following (1)

$$f_{ZC}(x_i, x_{i+1}) = \begin{cases} 1, x_i < 0 \text{ and } x_{i+1} > 0 \\ or x_i > 0 \text{ and } x_{i+1} < 0 \\ 0, otherwise \end{cases} \quad (1)$$

This method is considered straightforward as it involves the comparison of two continuous samples to ascertain the presence or absence of a zero crossover [33]. Now, the ZCR was calculated using (2) inside the sliding window in the manner described below

$$Z = \frac{f_{ZC}(x_i, x_{i+1})}{L} \quad (2)$$

L is the length of the window. According to Mikkelsen et al. the duration of contractions is generally 61.0 ± 18.0 sec (mean SD) [34] in the EHG signal. In this study we used the length of the window 120 sec to cover an EHG segment of contraction and move the window one step to the right. Here, we employed the sliding window to eliminate the requirement for loop reuse and optimize the program. Calculate the number of samples in each window using (3)

$$number\ of\ samples = L * f_s \quad (3)$$

2) INTERPOLATED NORMALIZED POWER OF ZCR

Following the acquisition of the zero-crossing rate, we computed the power of ZCR or ZCR^y. In this case, y is set to 1.2 to increase the larger values and decrease the smaller values of ZCR. EHG burst would strengthen and the non-UC segment's influence would be lessened in this way. The goal of normalization is to change the values of numeric columns in the dataset to a common scale, without distorting differences in the ranges of values. Next, without distorting the disparities in the ranges of values, the power of ZCR was normalized to convert the values of the dataset's numeric columns to a single scale (0 to 1). Here, linear interpolation has been used to match the sample number of the original signal with the normalized power of ZCR.

3) MODULATION TECHNIQUE

Now we applied the amplitude modulation technique on the pre-processed EHG signal and the power of Zero crossing rate shown in Fig. 4. The modulated signal is obtained using the following formula

$$\text{Modulated signal} = \text{preprocessed EHG}^*(\text{ZCR}^y)$$

Amplitude modulation is commonly used in transmitting a piece of information through a carrier signal. To protect against signal quality degradation and prevent information loss, it is essential to have a modulation index greater than 1. This can be represented as follows.

$$\begin{aligned} &\text{The modulation index} \\ &= \text{modulating signal/carrier signal} \\ &= (A_{\text{Power of ZCR}}/A_{\text{EHG}}) \end{aligned}$$

where $A_{\text{Power of ZCR}}$ = amplitude of power of ZCR signal, A_{EHG} = amplitude of preprocessed EHG signal, and here the obtained value of m is greater than 1.

4) ENVELOPE DETECTION USING RMS

The application of Root Mean Square (RMS) in obtaining the envelope of the electrohysterogram signal offers a practical and straightforward solution for online analysis [35]. The envelope of the modulated EHG signal was obtained by RMS using (4)

$$RMS = \sqrt{\frac{1}{N}} \sum_{i=0}^{N-1} x_i^2 \quad (4)$$

In this case, N denotes the length of the 40-second EHG segment where N= 40*fs (8000 points), and x_i is the amplitude of the modulated EHG signal at point i.

5) RECOGNITION OF UCS USING THRESHOLD (TH)

Finally, we set a threshold level to extract the uterine contractions which is given in (5) [36].

$$Threshold = 1.2 * (basetone + 0.15 * (signal\ range)) \quad (5)$$

where Basal tone = mean of 10% of the lowest values. If the sample value > th and is true for ≥ 30 seconds, then it is identified as a contraction otherwise consider it as a non-contraction segment.

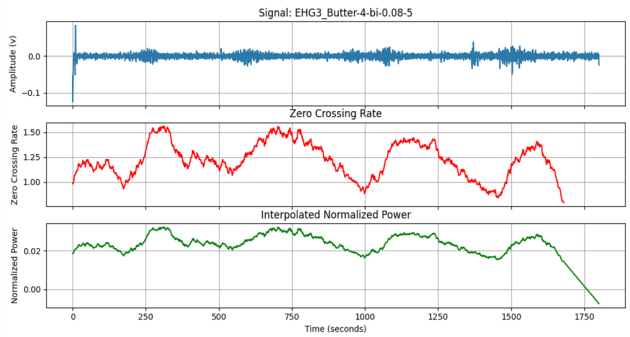

FIGURE 4. The top plot is the preprocessed EHG3 signal (record tpehgt_P010), 2nd plot is the zero-crossing rate of the preprocessed signal, and the bottom plot is interpolated normalized power of ZCR.

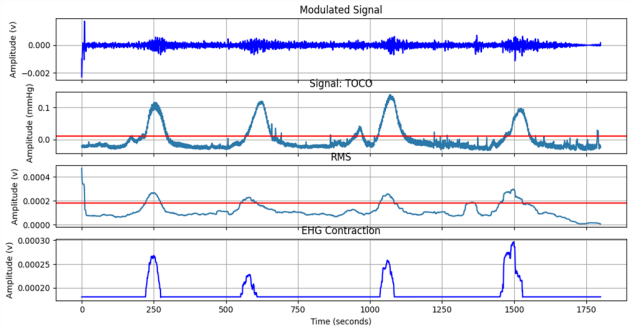

FIGURE 5. The top plot is modulated EHG3 signal (record tpehgt_P010), 2nd plot is the TOCO signal, 3rd plot is RMS value of the modulated signal and the bottom plot is extracted contraction segments.

The normal base tone of uterine contraction varies from 10 to 30 mmHg [37]. This baseline of the uterine contraction is required to identify the contraction duration and contraction strength. For the TOCO signal shown in Fig. 5 (2nd plot from the top), the threshold value was selected as 10 mmHg [38]. In that case, contractions were identified when the amplitude value is greater than the threshold value.

6) CONSISTENCY MEASUREMENT OF EXTRACTED UTERINE CONTRACTION

In our study, we utilized the Contractions Consistency Index (CCI) to explore the relationship between the extracted uterine contractions from EHG and the TOCO signal. This approach enables the determination of timing parameters for specific contractions that are consistently identified through the examination of both signals. In evaluating the consistency contractions, we utilized the formula (6) for the Contractions Consistency Index as defined by Jezewski et al. [39].

$$CCI = \frac{N_C}{\frac{1}{2}(N_T + N_{E)}} \tag{6}$$

In this equation, N_T is the number of contractions detected in the TOCO signal, N_E is the number of contractions detected in the EHG signal and N_C is the number of consistent contractions. Electrical excitation of myometrium cells serves as an initiating factor, with mechanical contraction being the ensuing outcome. The onset of mechanical contraction

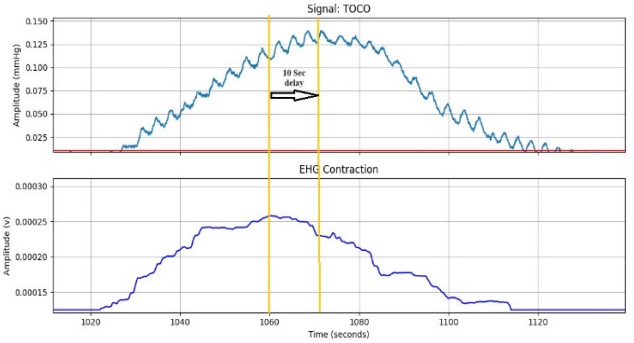

FIGURE 6. Consistency between contractions extracted from TOCO (upper plot) and EHG (lower plot).

commences subsequent to the cell entering the depolarization phase. Consequently, it is reasonable to anticipate that electrical activity precedes the mechanical contraction, and the maximum action potential is expected to occur in conjunction with the ascending phase of the contraction. Conversely, the propagation of excitation within the uterus is uncertain, and the timeframe required for excitation to reach the electrode measurement area may exhibit variability. In this context, consistent contractions were defined by the temporal difference between the maximum peak of the contraction in the EHG signal and the corresponding contraction detected by TOCO, which had to fall within a range of ±60 seconds [40]. If an equal number of contractions are detected in both signals, and all of them are confirmed to be consistent, the index is regarded as 1 in such instances.

D. FEATURE EXTRACTION

Each feature in our investigation was only calculated for the contraction segments that were extracted, not for the entire EHG signals. The following features were chosen to be the most often employed in EHG-based pregnancy monitoring and preterm risk evaluation research algorithms:

1) ENERGY

The energy of a given discrete signal x is computed as the sum of the squared x values over the n samples. The units are Volt^2

$$Energy = \sum_{i=1}^{n} x_i^2$$

2) CONTRACTION INTENSITY

It is quantified by assessing the count of positive and negative peaks within a 40-second interval.

$$contraction\ intensity = \frac{total\ number\ of\ positive\ and\ negative\ peaks}{2} * \frac{40}{T_D}$$

Here, T_D is the duration of the identified contraction in seconds which is computed by taking the difference between the automatically detected contractions' onset and offset samples.

3) MEAN FREQUENCY

It is the estimation of the mean of the normalized frequency of the power spectrum [41]. It is defined as:

$$f_{mean} = \frac{\sum_{i=1}^{M} f_i p_i}{\sum_{i=1}^{M} p_i}$$

Here, f_i is the frequency value and p_i is the amplitude of the Power spectrum density component.

4) MEDIAN FREQUENCY

$$f_{med} = \sum_{i=j}^{M} p\,(i)$$

p_i is the i-th Power spectrum density component. M is the number of frequency components in PSD and j is the j-th PSD component

5) PEAK TO PEAK AMPLITUDE

Peak-to-peak amplitude was calculated by measuring the change between peak (highest amplitude value) and trough (lowest amplitude value) which is expressed as

$$pk\ to\ pk = |max_x - min_x|$$

6) SHANON ENTROPY

Shannon entropy [42] represents the average rate at which information is generated by a stochastic source of data. A higher Shannon entropy indicates a greater amount of information conveyed by a new value in the data-generating process.

$$Shanon\ En = \sum_{i=1}^{n} x_i^2 log\ x_i^2$$

7) SAMPLE ENTROPY

Entropy serves as an evaluative metric for the intricacy of physiological time series -EHG signal [43]:

$$Sample\ En = \left\{ \begin{array}{c} -log \frac{c_m}{c_{m-1}}, c_m \neq 0 \cap c_{m-1} \neq 0 \\ -log \frac{N-m}{N-m-1}, c_m = 0 \cap c_{m-1} = 0 \end{array} \right\}$$

where, N = length of the time series, m = the length of the sequences to be compared, r = the tolerance for accepting matches, and cm = the number of patterns matches (within a margin for r) that is constructed for each m.

8) LOG DETECTOR

It is the time domain linear feature which is expressed as:

$$\text{log detector} = e^{1/N \sum_{i=1}^{N} \log|x(i)|}$$

E. CLASSIFICATION

The dataset utilized in this study exhibits an imbalance in terms of sample size between term deliveries, representing the majority class with 281 records, and preterm deliveries, representing the minority class with 57 records. This imbalance can potentially introduce bias in classification models, as classifiers tend to be more sensitive to the majority class and less sensitive to the minority class [44]. In this study, SMOTE (Synthetic Minority Over-sampling Technique) was employed to oversample the minority class (preterm), thereby addressing the class imbalance and achieving a balanced representation of term and preterm samples in the dataset.

In this study, RF was employed as a classifier due to its simplicity and diversity. To assess the random forest (RF) classifier performance for identifying preterm and term delivery, a five-fold cross-validation approach was used. One subset was utilized to test the RF, and five subsets were used to train it based on the attributes of the term group and preterm, respectively. The five subsets were utilized once each as test data throughout the cross-validation process. The performance of the RF classification results was assessed by averaging the accuracy (ACC), sensitivity, and precision from the fivefold cross-validation. For this classifier, the split data ratio was 70% for training to 30% for testing.

Here, the Accuracy (ACC), Sensitivity/Recall, and Precision were calculated as follows [45]:

$$\begin{aligned} \text{ACC} &= \text{TP} + \text{TN}/\text{FP} + \text{TN} + \text{TP} + \text{FN} \\ \text{Sensitivity}/ &= \text{TP}/\text{TP} + \text{FN} \\ \text{precision} &= \text{TP}/\text{TP} + \text{FP} \end{aligned}$$

where TP (true positives) and TN (true negatives) are the numbers of UC segments of term and preterm EHG that were correctly classified, and FP (false positives) and FN (false negatives) are the numbers of UC segments of term and preterm EHG that were falsely classified. The results of ACC, Sensitivity, and precision from the five-fold cross-validation were calculated and averaged to evaluate the RF classifier.

IV. RESULTS

In Fig. 6, the upper plot depicts uterine contraction based on the TOCO signal, while the lower plot represents contraction based on the Electromyogram (EHG). Here we observed that the EHG contraction precedes the mechanical contraction by 30 s which aligns with the reference provided earlier in the text. This concurrent pattern allows us to categorize both contractions as consistently aligned.

$$\begin{aligned} \text{ACC} &= \text{TP} + \text{TN}/\text{FP} + \text{TN} + \text{TP} + \text{FN} = 89\% \\ \text{Sensitivity/recall} &= \text{TP}/\text{TP} + \text{FN} = 85.87\% \\ \text{precision} &= \text{TP}/\text{TP} + \text{FP} = 88.76\% \end{aligned}$$

The investigation, detailed across Tables 1 and 2, delves into the Contraction consistency Index (CCI) across subjects in both term and pre-term conditions. In Table 1, contractions were identified utilizing mean amplitude threshold criteria, a method specified by Song et al. [18]. Within the preterm condition, 65 contractions were consistently recognized among the 13 subjects, compared to 71 consistent contractions observed in all 13 subjects within the term condition. The CCI index, computed using equation (6), was then

TABLE 1. CCI of subjects in Term condition and pre-term condition (Based on mean amplitude threshold criteria [18]).

Subject no (In pre-term condition)	Contraction's number in TOCO (N_T)	Contraction's number in EHG (N_E)	Consistent contraction number (N_C)	CCI	Subject no (In term condition)	Contraction's number in TOCO (N_T)	Contraction's number in EHG (N_E)	Consistent contraction number (N_C)	CCI
Tpehgt_p001	**3**	**2**	2	0.8	Tpehgt_t001	**3**	**3**	**3**	1
Tpehgt_p002	**12**	**16**	12	0.85	Tpehgt_t002	**9**	**7**	**7**	0.87
Tpehgt_p003	**3**	**1**	1	0.5	Tpehgt_t003	**8**	**9**	**8**	0.94
Tpehgt_p004	**6**	**5**	5	0.91	Tpehgt_t004	**4**	**3**	**3**	0.85
Tpehgt_p005	**5**	**5**	5	1	Tpehgt_t005	**6**	**9**	**6**	0.8
Tpehgt_p006	**7**	**7**	7	1	Tpehgt_t006	**4**	**6**	**4**	0.8
Tpehgt_p007	**7**	**4**	4	0.72	Tpehgt_t007	**4**	**2**	**2**	0.66
Tpehgt_p008	**6**	**5**	5	0.91	Tpehgt_t008	**5**	**6**	**5**	0.90
Tpehgt_p009	**9**	**6**	6	0.8	Tpehgt_t009	**3**	**5**	**3**	0.75
Tpehgt_p010	**2**	**1**	1	0.66	Tpehgt_t010	**8**	**5**	**5**	0.77
Tpehgt_p011	**15**	**11**	11	0.85	Tpehgt_t011	**12**	**10**	**10**	0.90
Tpehgt_p012	**6**	**3**	3	0.67	Tpehgt_t012	**9**	**9**	**9**	1
Tpehgt_p013	**2**	**4**	2	0.66	Tpehgt_t013	**7**	**6**	**6**	0.92
Avg			64	**0.79**				**71**	**0.86**

reported for both groups, revealing an average CCI index of 0.79 during pre-term conditions and 0.86 during term conditions.

In Table 2, a parallel assessment was conducted, albeit with contractions detected using proposed threshold criteria. Notably, among the 13 subjects in the pre-term condition, 75 contractions were identified as consistent, while 77 consistent contractions were recognized across all 13 subjects in the term condition. Subsequently, the CCI index was calculated using the same methodology as in Table 2, yielding an average CCI index of 0.91 during pre-term conditions and 0.90 during term conditions.

V. DISCUSSION

Manual identification of contractions is labor-intensive and necessitates specialized personnel for operation. Therefore, it is imperative to develop automatic recognition systems for locating contractions, particularly in an era where wearable and wireless devices garner significant attention. Using additional electrodes in uterine activity monitoring can offer a more comprehensive understanding of uterine dynamics, providing abundant information for analysis. However, the increased number of electrodes may introduce practical challenges in clinical settings [46]. Based on the literature analysis, it was found that 16 electrode configurations were the most commonly used by researchers, with 8 electrode configurations being used sporadically for automatic uterine contraction detection. Hence, it is imperative to explore the effects of the four-electrode configuration on uterine contraction (UC) recognition. Our efforts in this work can contribute to optimizing electrode arrangement, potentially leading to the need for fewer electrodes while extracting valuable and meaningful information from uterine contractions. This optimization process aims to streamline uterine activity monitoring, making it more feasible and efficient for routine clinical practice. In our study, we utilized the EHG signal acquired from a 4-electrode configuration, focusing on the bottom horizontal position of the uterus (channel 3).

TABLE 2. CCI of subjects in Term condition and pre-term condition (Based on proposed threshold criteria).

Subject no (In pre-term condition)	Contraction's number in TOCO (N_T)	Contraction's number in EHG (N_E)	Consistent contraction number (N_C)	CCI	Subject no (In term condition)	Contraction's number in TOCO (N_T)	Contraction's number in EHG (N_E)	Consistent contraction number (N_C)	CCI
Tpehgt_p001	**3**	**3**	3	1	Tpehgt_t001	**3**	**3**	**3**	1
Tpehgt_p002	**12**	**15**	12	0.89	Tpehgt_t002	**9**	**8**	**8**	0.94
Tpehgt_p003	**3**	**3**	3	1	Tpehgt_t003	**8**	**9**	**8**	0.94
Tpehgt_p004	**6**	**6**	6	1	Tpehgt_t004	**4**	**5**	**4**	0.89
Tpehgt_p005	**5**	**5**	5	1	Tpehgt_t005	**6**	**9**	**6**	0.8
Tpehgt_p006	**7**	**7**	7	1	Tpehgt_t006	**4**	**6**	**4**	0.8
Tpehgt_p007	**7**	**8**	7	0.93	Tpehgt_t007	**4**	**4**	**4**	1
Tpehgt_p008	**6**	**6**	6	1	Tpehgt_t008	**5**	**5**	**5**	1
Tpehgt_p009	**9**	**8**	7	0.82	Tpehgt_t009	**3**	**5**	**3**	0.75
Tpehgt_p010	**2**	**1**	1	0.67	Tpehgt_t010	**8**	**6**	**4**	0.57
Tpehgt_p011	**15**	**12**	12	0.89	Tpehgt_t011	**12**	**12**	**12**	1
Tpehgt_p012	**6**	**4**	4	0.8	Tpehgt_t012	**9**	**9**	**9**	1
Tpehgt_p013	**2**	**3**	2	0.8	Tpehgt_t013	**7**	**7**	**7**	1
Avg			**75**	**0.91**				**77**	**0.9**

However, due to the lack of uniformity in evaluation metrics across published works [15], [16], [17], [18] pertaining to contraction detection, and the predominant utilization of private databases in these experiments, direct comparisons of their results are inherently challenging. To facilitate a more coherent comparison, we opted to apply the threshold method outlined by X to our database. Analysis of Table 2 reveals that through the application of a proposed threshold-based criterion, we successfully extracted contractions, achieving a CCI index of 91% for preterm births and 82% for term births. This observation underscores a noteworthy advancement, as evidenced by the examination of Tables 1 and 2, where our study demonstrates a superior Contraction consistency Index (CCI) compared to previous research.

Following the acquisition of the high CCI index, we applied this amplitude modulation-based approach to 300 TPEHG DB records. From these records, we retrieved 167 contraction segments from preterm data (38 recordings) and 706 contraction segments from term data (262 records). To identify normal and premature births, we are now extracting information from a total of 1021 contraction segments. J. D. Iams et al.'s research findings indicate that measuring the frequency and number of uterine contractions lacks clinical utility in predicting preterm delivery [47]. Consequently, our efforts have shifted towards extracting well-known features from contraction bursts as a means of predicting preterm birth. Numerous researchers have undertaken the task of extracting diverse features from entire EHG signals, employing them as inputs for classifiers aimed at discerning preterm birth and the mode of delivery. Effective features from the linear, non-linear, and temporal-frequency domains have been shown to be essential for improving classifier performance and reducing computational expenses at the same time. The previous studies concluded that nonlinear methods such as sample entropy [48], [49], approximate entropy [49], [50], and Shannon entropy [51] can provide better discrimination between pregnancy and labor contractions compared to linear methods [52]. It is probably because entropy reflects

TABLE 3. Statistical significance of the EHG features from extracted contractile episode. Bold indicating significant difference.

Signal Feature	Standard Error	P-value
Energy	0.000055061	<.001
Contraction intensity	0.003887693	0.012
Contraction duration	0.00006676	0.030
Mean frequency	0.002684509	.331
Median frequency	0.000875351	.117
Pk to pk amplitude	0.00002066	.014
Shanon entropy	0.001108986	<.001
Sample entropy	0.000039652	.108
Log detector	0.000199906	.001

TABLE 4. Confusion matrix of RF classifier.

	Classified term	Classified pre-term
Term	79	13
Pre-term	10	188

ACC = TP +TN/FP+TN + TP+FN =89%

Sensitivity/recall = TP/ TP+ FN=85.87%

precision=TP/ TP+ FP=88.76%

the complex and nonlinear dynamic interactions between myometrium cells [24]. In our study, we extracted five time-domain features—namely, energy, peak-to-peak amplitude, contraction intensity, and contraction duration, log detector—that collectively constitute the conventional characterization of electrohysterogram (EHG) contraction segments. The results in Table 3 showed that these features give a significant difference (p-value <0.05) between term and preterm EHG. This statistical assessment was conducted using the non-parametric Mann–Whitney U-test, with a significance level of $p<0.05$. This result shows some agreement with the one reported for uterine contractions by Martim et al. [53], where peak to peak amplitude parameter has been found to significantly increase with gestational age. However, according to their study, when labor approaches, energy and Shannon entropy increase. Additionally, these features did not show dependency on the anthropometric variables (height, weight, head circumference, body mass index (BMI), body circumferences to assess for adiposity (waist, hip, and limbs), and skinfold thickness) [54]. Therefore, in addition to these classical parameters related to contractile activity, entropy indices were extracted from contraction segments to assess the efficacy of the method in classifying between normal and premature births. Recently, several academics have concentrated on entropy-based indices as a means of evaluating and quantifying the complexity of EHG time series [55], [56], [57], [58], [59]. Most of the researchers suggested that for predicting preterm labor and assessing the progress of labor efficiently it would be better to choose sample entropy and median frequency as potential features. In our analysis, the sample entropy did not exhibit the same capability as reported earlier, which suggested a significant distinction between the preterm and term signals, when it was computed for the contractile episodes alone. Furthermore, as demonstrated by Krzysztof Horoba et al., the EHG 1 signal (located at the top horizontal electrode position) proved to be valuable for assessing the median frequency. In our study, we utilized the EHG 3 signal, which may not yield any discernible differences between term and preterm EHG signals when considering this particular characteristic. Another potential reason for this observation could be attributed to our approach of extracting contraction segments based on the time domain. Consequently, the frequency domain features failed to demonstrate any significant differences between the two classes. Finally, we incorporated six distinct features—namely energy, peak-to-peak amplitude, contraction intensity, contraction duration, log detector, and Shannon entropy—as input variables for the Random Forest (RF) classifier. The results, as illustrated in Table 4, depict the confusion matrix for this model. The corresponding performance metrics reveal an accuracy of 89%, sensitivity of 85.87%, and precision of 88.76%.

The study's findings suggest promising potential in distinguishing between preterm spontaneous delivery and term spontaneous delivery through algorithm-driven automated detection of uterine contractions. Future analyses will expand to include additional delivery types, such as induced and cesarean sections, utilizing a similar methodology to extract relevant information. Moreover, due to the absence of invasive IUPC, a comprehensive comparison between the contraction recognition approach and simultaneously recorded Intrauterine Pressure Catheter (IUPC) data was not feasible. IUPCs are known for their superior accuracy in determining the frequency and strength of uterine contractions compared to external tocodynamometry [60]. Hence, future analysis will evaluate the CCI index using IUPC data to verify the method.

VI. CONCLUSION

In conclusion, the study has demonstrated the effectiveness of utilizing the Root Mean Square (RMS) and Zero Crossing Rate (ZCR) technique, with a simple threshold-based rule, for accurately detecting uterine contractions from electrohysterogram (EHG) signals. Importantly, this approach utilized a reduced number of electrodes, enhancing efficiency and applicability in clinical settings. Moreover, the significance of

contraction segment attributes, particularly energy, peak-to-peak amplitude, contraction intensity, contraction duration, log detector, and Shannon entropy, has been demonstrated as paramount in distinguishing between full-term and preterm classifications. By employing this method, the detection of uterine contractions (UCs) may provide a direct pathway for automatically predicting preterm birth and labor outcome. Such advancements hold significant potential for enhancing obstetric care and maternal-fetal health management.

REFERENCES

[1] P. Li, L. Wang, X. Qian, A. Morse, R. E. Garfield, and H. Liu, "A study of uterine inertia on the spontaneous of labor using uterine electromyography," *Taiwanese J. Obstetrics Gynecol.*, vol. 60, no. 3, pp. 449–453, May 2021, doi: 10.1016/j.tjog.2021.03.010.

[2] R. L. Olmos-Ramírez, M. Á. Peña-Castillo, H. Mendieta-Zerón, and J. J. Reyes-Lagos, "Uterine activity modifies the response of the fetal autonomic nervous system at preterm active labor," *Frontiers Endocrinol.*, vol. 13, Jan. 2023, Art. no. 1056679, doi: 10.3389/fendo.2022.1056679.

[3] *Born too Soon: The Global Action Report on Preterm Birth*, World Health Organization, Geneva, Switzerland, 2012.

[4] K. Treyvaud, K. J. Lee, L. W. Doyle, and P. J. Anderson, "Very preterm birth influences parental mental health and family outcomes seven years after birth," *J. Pediatrics*, vol. 164, no. 3, pp. 515–521, Mar. 2014, doi: 10.1016/j.jpeds.2013.11.001.

[5] P. C. A. M. Bakker, M. Zikkenheimer, and H. P. van Geijn, "The quality of intrapartum uterine activity monitoring," *J. Perinatal Med.*, vol. 36, no. 3, pp. 197–201, Jan. 2008, doi: 10.1515/jpm.2008.027.

[6] C. M. Steer and G. J. Hertsch, "Electrical activity of the human uterus in labor: The electrohysterograph," *Amer. J. Obstetrics Gynecol.*, vol. 59, no. 1, pp. 25–40, Jan. 1950.

[7] F. Jager, S. Libenšek, and K. Geršak, "Characterization and automatic classification of preterm and term uterine records," *PLoS ONE*, vol. 13, no. 8, Aug. 2018, Art. no. e0202125, doi: 10.1371/journal.pone.0202125.

[8] D. Hao, J. Peng, Y. Wang, J. Liu, X. Zhou, and D. Zheng, "Evaluation of convolutional neural network for recognizing uterine contractions with electrohysterogram," *Comput. Biol. Med.*, vol. 113, Oct. 2019, Art. no. 103394, doi: 10.1016/j.compbiomed.2019.103394.

[9] C. K. Marque, J. Terrien, S. Rihana, and G. Germain, "Preterm labour detection by use of a biophysical marker: The uterine electrical activity," *BMC Pregnancy Childbirth*, vol. 7, no. S1, p. S5, Jun. 2007, doi: 10.1186/1471-2393-7-s1-s5.

[10] K. Horoba, J. Jezewski, A. Matonia, J. Wrobel, R. Czabanski, and M. Jezewski, "Early predicting a risk of preterm labour by analysis of antepartum electrohysterograhic signals," *Biocybern. Biomed. Eng.*, vol. 36, no. 4, pp. 574–583, 2016, doi: 10.1016/j.bbe.2016.06.004.

[11] A. Diab, S. Boudaoud, B. Karlsson, and C. Marque, "Performance comparison of coupling-evaluation methods in discriminating between pregnancy and labor EHG signals," *Comput. Biol. Med.*, vol. 132, May 2021, Art. no. 104308, doi: 10.1016/j.compbiomed.2021.104308.

[12] L. Chen and H. Xu, "Deep neural network for semi-automatic classification of term and preterm uterine recordings," *Artif. Intell. Med.*, vol. 105, May 2020, Art. no. 101861, doi: 10.1016/j.artmed.2020.101861.

[13] Z. Liu, D. Hao, L. Zhang, J. Liu, X. Zhou, L. Yang, Y. Yang, X. Li, S. Zhang, and D. Zheng, "Comparison of electrohysterogram characteristics during uterine contraction and non-contraction during labor," in *Proc. 39th Annu. Int. Conf. IEEE Eng. Med. Biol. Soc. (EMBC)*, Jeju, South Korea, Jul. 2017, pp. 2924–2927, doi: 10.1109/EMBC.2017.8037469.

[14] H. Rosen and Y. Yogev, "Assessment of uterine contractions in labor and delivery," *Amer. J. Obstetrics Gynecol.*, vol. 28, no. 5, pp. S1209–S1221, Mar. 2023, doi: 10.1016/j.ajog.2022.09.003.

[15] F. Esgalhado, A. G. Batista, H. Mouriño, S. Russo, C. R. P. dos Reis, F. Serrano, V. Vassilenko, and M. D. Ortigueira, "Automatic contraction detection using uterine electromyography," *Appl. Sci.*, vol. 10, no. 20, p. 7014, Oct. 2020, doi: 10.3390/app10207014.

[16] C. Muszynski, T. Happillon, K. Azudin, J.-B. Tylcz, D. Istrate, and C. Marque, "Automated electrohysterographic detection of uterine contractions for monitoring of pregnancy: Feasibility and prospects," *BMC Pregnancy Childbirth*, vol. 18, no. 1, p. 136, May 2018, doi: 10.1186/s12884-018-1778-1.

[17] Z. Chen, M. Wang, M. Zhang, W. Huang, Y. Feng, and J. Xu, "Automatic detection and characterization of uterine contraction using electrohysterography," *Biomed. Signal Process. Control*, vol. 90, Apr. 2024, Art. no. 105840, doi: 10.1016/j.bspc.2023.105840.

[18] X. Song, X. Qiao, D. Hao, L. Yang, X. Zhou, Y. Xu, and D. Zheng, "Automatic recognition of uterine contractions with electrohysterogram signals based on the zero-crossing rate," *Sci. Rep.*, vol. 11, no. 1, p. 1956, Jan. 2021, doi: 10.1038/s41598-021-81492-1.

[19] J. Peng, D. Hao, H. Liu, J. Liu, X. Zhou, and D. Zheng, "Preliminary study on the efficient electrohysterogram segments for recognizing uterine contractions with convolutional neural networks," *BioMed Res. Int.*, vol. 2019, pp. 1–9, Oct. 2019, doi: 10.1155/2019/3168541.

[20] D. Schlembach, W. Maner, R. Garfield, and H. Maul, "Monitoring the progress of pregnancy and labor using electromyography," *Eur. J. Obstetrics Gynecol. Reproductive Biol.*, vol. 144, pp. 33–39, May 2009, doi: 10.1016/j.ejogrb.2009.02.016.

[21] L. Miha, J. Ruben, R. Linda, L. William, S. Shao-Qing, S. Leili, B. James, and E. Robert, "Use of uterine electromyography to diagnose term and preterm labor," *Acta Obstetricia et Gynecol. Scandinavica*, vol. 90, no. 2, pp. 150–157, 2011, doi: 10.1111/j.1600-0412.2010.01031.x.

[22] M. Lucovnik, W. L. Maner, L. R. Chambliss, R. Blumrick, J. Balducci, Z. Novak-Antolic, and R. E. Garfield, "Noninvasive uterine electromyography for prediction of preterm delivery," *Amer. J. Obstetrics Gynecol.*, vol. 204, no. 3, p. 228, Mar. 2011, doi: 10.1016/j.ajog.2010.09.024.

[23] A. Alexandersson, T. Steingrimsdottir, J. Terrien, C. Marque, and B. Karlsson, "The Icelandic 16-electrode electrohysterogram database," *Sci. Data*, vol. 2, no. 1, Apr. 2015, Art. no. 150017, doi: 10.1038/sdata.2015.17.

[24] G. Fele-Žorž, G. Kavšek, Ž. Novak-Antolič, and F. Jager, "A comparison of various linear and non-linear signal processing techniques to separate uterine EMG records of term and pre-term delivery groups," *Med. Biol. Eng. Comput.*, vol. 46, no. 9, pp. 911–922, Apr. 2008, doi: 10.1007/s11517-008-0350-y.

[25] V. Shulgin and O. Shepel, "Electrohysterographic signals processing for uterine activity detection and characterization," in *Proc. IEEE 34th Int. Sci. Conf. Electron. Nanotechnol. (ELNANO)*, Kyiv, Ukraine, Apr. 2014, pp. 269–272, doi: 10.1109/ELNANO.2014.6873918.

[26] N. V. Iqbal and K. Subramaniam, "Robust feature sets for contraction level invariant control of upper limb myoelectric prosthesis," *Biomed. Signal Process. Control*, vol. 51, pp. 90–96, May 2019, doi: 10.1016/j.bspc.2019.02.010.

[27] J. Shen, Y. Liu, M. Zhang, A. Pumir, L. Mu, B. Li, and J. Xu, "Multi-channel electrohysterography enabled uterine contraction characterization and its effect in delivery assessment," *Comput. Biol. Med.*, vol. 167, Dec. 2023, Art. no. 107697, doi: 10.1016/j.compbiomed.2023.107697.

[28] G. Gaudet, M. Raison, and S. Achiche, "Classification of upper limb phantom movements in transhumeral amputees using electromyographic and kinematic features," *Eng. Appl. Artif. Intell.*, vol. 68, pp. 153–164, Feb. 2018, doi: 10.1016/j.engappai.2017.10.017.

[29] G. Huang, Z. Xian, Z. Zhang, S. Li, and X. Zhu, "Divide-and-conquer muscle synergies: A new feature space decomposition approach for simultaneous multifunction myoelectric control," *Biomed. Signal Process. Control*, vol. 44, pp. 209–220, Jul. 2018.

[30] N. Jiang, T. Lan, F. Peng, Y. Dai, and G. Li, "Motion recognition for simultaneous control of multifunctional transradial prostheses," in *Proc. 35th Annu. Int. Conf. IEEE Eng. Med. Biol. Soc. (EMBC)*, Jul. 2013, pp. 1603–1606, doi: 10.1109/EMBC.2013.6609822.

[31] A. Phinyomark, F. Quaine, S. Charbonnier, C. Serviere, F. Tarpin-Bernard, and Y. Laurillau, "EMG feature evaluation for improving myoelectric pattern recognition robustness," *Expert Syst. Appl.*, vol. 40, no. 12, pp. 4832–4840, Sep. 2013, doi: 10.1016/j.eswa.2013.02.023.

[32] N. Rudhakrishnan, J. D. Wilson, C. Lowery, H. Eswaran, and P. Murphy, "A fast algorithm for detecting contractions in uterine electromyography," *IEEE Eng. Med. Biol. Mag.*, vol. 19, no. 2, pp. 89–94, Mar. 2000, doi: 10.1109/51.827411.

[33] D. C. Toledo-Pérez, J. Rodríguez-Reséndiz, and R. A. Gómez-Loenzo, "A study of computing zero crossing methods and an improved proposal for EMG signals," *IEEE Access*, vol. 8, pp. 8783–8790, 2020, doi: 10.1109/ACCESS.2020.2964678.
[34] E. Mikkelsen, P. Johansen, A. Fuglsang-Frederiksen, and N. Uldbjerg, "Electrohysterography of labor contractions: Propagation velocity and direction," *Acta Obstetricia et Gynecol. Scandinavica*, vol. 92, no. 9, pp. 1070–1078, Jul. 2013, doi: 10.1111/aogs.12190.
[35] C. Rabotti, M. Mischi, J. O. E. H. van Laar, G. S. Oei, and J. W. M. Bergmans, "Estimation of internal uterine pressure by joint amplitude and frequency analysis of electrohysterographic signals," *Physiol. Meas.*, vol. 29, no. 7, pp. 829–841, Jun. 2008, doi: 10.1088/0967-3334/29/7/011.
[36] S. N. Vasist, P. Bhat, S. Ulman, and H. Hebbar, "Identification of contractions from Electrohysterography for prediction of prolonged labor," *J. Elect. Bioimpedance*, vol. 13, no. 1, pp. 4–9, Jan. 2022, doi: 10.2478/joeb-2022-0002.
[37] D. Hao, Q. Qiu, X. Zhou, Y. An, J. Peng, L. Yang, and D. Zheng, "Application of decision tree in determining the importance of surface electrohysterography signal characteristics for recognizing uterine contractions," *Biocybern. Biomed. Eng.*, vol. 39, no. 3, pp. 806–813, Jul. 2019, doi: 10.1016/j.bbe.2019.06.008.
[38] R. Parameshwari and S. S. Devi, "Acquisition and analysis of electrohysterogram signal," *J. Med. Syst.*, vol. 44, no. 3, Feb. 2020, doi: 10.1007/s10916-020-1523-y.
[39] J. Jezewski, K. Horoba, A. Matonia, and J. Wrobel, "Quantitative analysis of contraction patterns in electrical activity signal of pregnant uterus as an alternative to mechanical approach," *Physiol. Meas.*, vol. 26, no. 5, pp. 753–767, Jul. 2005, doi: 10.1088/0967-3334/26/5/014.
[40] T. Y. Euliano, M. T. Nguyen, D. Marossero, and R. K. Edwards, "Monitoring contractions in obese parturients," *Obstetrics Gynecol.*, vol. 109, no. 5, pp. 1136–1140, May 2007, doi: 10.1097/01.aog.0000258799.24496.93.
[41] D. Alamedine. (Jul. 21, 2015). *Selection of EHG Parameter Characteristics for the Classification of Uterine Contractions*. Semantic Scholar. Accessed: Dec. 4, 2023. [Online]. Available: https://api.semanticscholar.org/CorpusID:110696974
[42] A. A. Torres-García, O. Mendoza-Montoya, M. Molinas, J. M. Antelis, L. A. Moctezuma, and T. Hernández-Del-Toro, "Pre-processing and feature extraction," in *Biosignal Processing and Classification Using Computational Learning and Intelligence*, 2022, pp. 59–91, doi: 10.1016/b978-0-12-820125-1.00014-2.
[43] J. S. Richman and J. R. Moorman, "Physiological time-series analysis using approximate entropy and sample entropy," *Amer. J. Physiol.-Heart Circulatory Physiol.*, vol. 278, no. 6, pp. H2039–H2049, Jun. 2000, doi: 10.1152/ajpheart.2000.278.6.h2039.
[44] I. Dey and V. Pratap, "A comparative study of SMOTE, borderline-SMOTE, and ADASYN oversampling techniques using different classifiers," in *Proc. 3rd Int. Conf. Smart Data Intell. (ICSMDI)*, Trichy, India, Mar. 2023, pp. 294–302, doi: 10.1109/ICSMDI57622.2023.00060.
[45] M. P. G. C. Vinken, C. Rabotti, M. Mischi, and S. G. Oei, "Accuracy of frequency-related parameters of the electrohysterogram for predicting preterm delivery," *Obstetrical Gynecol. Surv.*, vol. 64, no. 8, pp. 529–541, Aug. 2009, doi: 10.1097/ogx.0b013e3181a8c6b1.
[46] D. Hao, X. Song, Q. Qiu, X. Xin, L. Yang, X. Liu, H. Jiang, and D. Zheng, "Effect of electrode configuration on recognizing uterine contraction with electrohysterogram: Analysis using a convolutional neural network," *Int. J. Imag. Syst. Technol.*, vol. 31, no. 2, pp. 972–980, Oct. 2020, doi: 10.1002/ima.22505.
[47] J. D. Iams, R. B. Newman, E. A. Thom, R. L. Goldenberg, E. Mueller-Heubach, A. Moawad, B. M. Sibai, S. N. Caritis, M. Miodovnik, R. H. Paul, and M. P. Dombrowski, "Frequency of uterine contractions and the risk of spontaneous preterm delivery," *New England J. Med.*, vol. 346, no. 4, pp. 250–255, Jan. 2002, doi: 10.1056/nejmoa002868.
[48] A. Smrdel and F. Jager, "Separating sets of term and pre-term uterine EMG records," *Physiol. Meas.*, vol. 36, no. 2, pp. 341–355, Jan. 2015, doi: 10.1088/0967-3334/36/2/341.
[49] I. O. Idowu, P. Fergus, A. Hussain, C. Dobbins, M. Khalaf, R. V. C. Eslava, and R. Keight, "Artificial intelligence for detecting preterm uterine activity in gynecology and obstetric care," in *Proc. IEEE Int. Conf. Comput. Inf. Technol.; Ubiquitous Comput. Commun.; Dependable, Autonomic Secure Comput.; Pervasive Intell. Comput.*, Liverpool, U.K., Oct. 2015, pp. 215–220, doi: 10.1109/CIT/IUCC/DASC/PICOM.2015.31.
[50] S. M. Naeem, A. F. Seddik, and M. A. Eldosoky, "New technique based on uterine electromyography nonlinearity for preterm delivery detection," *J. Eng. Technol. Res.*, vol. 7, no. 6, pp. 14–107, 2014.
[51] P. Ren, S. Yao, J. Li, P. A. Valdes-Sosa, and K. M. Kendrick, "Improved prediction of preterm delivery using empirical mode decomposition analysis of uterine electromyography signals," *PLoS ONE*, vol. 10, no. 7, Jul. 2015, Art. no. e0132116, doi: 10.1371/journal.pone.0132116.
[52] H. Carola, A. S. Sherif, and R. Rodrigo, "Potential use of electrohysterography in obstetrics: A review article," *J. Maternal-Fetal Neonatal Med.*, vol. 34, no. 10, pp. 1666–1672, 2019, doi: 10.1080/14767058.2019.1639663.
[53] M. Almeida, H. Mouriño, A. G. Batista, S. Russo, F. Esgalhado, C. R. P. dos Reis, F. Serrano, and M. Ortigueira, "Electrohysterography extracted features dependency on anthropometric and pregnancy factors," *Biomed. Signal Process. Control*, vol. 75, May 2022, Art. no. 103556, doi: 10.1016/j.bspc.2022.103556.
[54] K. Casadei and J. Kiel. *Anthropometric Measurement*. Accessed: Mar. 24, 2019. [Online]. Available: https://www.ncbi.nlm.nih.gov/books/NBK537315/
[55] H. Romero-Morales, J. N. Muñoz-Montes de Oca, R. Mora-Martínez, Y. Mina-Paz, and J. J. Reyes-Lagos, "Enhancing classification of preterm-term birth using continuous wavelet transform and entropy-based methods of electrohysterogram signals," *Frontiers Endocrinol.*, vol. 13, Jan. 2023, Art. no. 1035615, doi: 10.3389/fendo.2022.1035615.
[56] F. Nieto-del-Amor, R. Beskhani, Y. Ye-Lin, J. Garcia-Casado, A. Diaz-Martinez, R. Monfort-Ortiz, V. J. Diago-Almela, D. Hao, and G. Prats-Boluda, "Assessment of dispersion and bubble entropy measures for enhancing preterm birth prediction based on electrohysterographic signals," *Sensors*, vol. 21, no. 18, p. 6071, Sep. 2021, doi: 10.3390/s21186071.
[57] J. J. Reyes-Lagos, A. C. Pliego-Carrillo, C. I. Ledesma-Ramírez, M. Á. Peña-Castillo, M. T. García-González, G. Pacheco-López, and J. C. Echeverría, "Phase entropy analysis of electrohysterographic data at the third trimester of human pregnancy and active parturition," *Entropy*, vol. 22, no. 8, p. 798, Jul. 2020, doi: 10.3390/e22080798.
[58] R. Zeng, Y. Lu, S. Long, C. Wang, and J. Bai, "Cardiotocography signal abnormality classification using time-frequency features and ensemble cost-sensitive SVM classifier," *Comput. Biol. Med.*, vol. 130, Mar. 2021, Art. no. 104218, doi: 10.1016/j.compbiomed.2021.104218.
[59] A. Cheng, Y. Yao, Y. Jin, C. Chen, R. Vullings, L. Xu, and M. Mischi, "Novel multichannel entropy features and machine learning for early assessment of pregnancy progression using electrohysterography," *IEEE Trans. Biomed. Eng.*, vol. 69, no. 12, pp. 3728–3738, Dec. 2022, doi: 10.1109/TBME.2022.3176668.
[60] T. Y. Euliano, M. T. Nguyen, S. Darmanjian, S. P. McGorray, N. Euliano, A. Onkala, and A. R. Gregg, "Monitoring uterine activity during labor: A comparison of 3 methods," *Amer. J. Obstetrics Gynecol.*, vol. 208, no. 1, p. 66, Jan. 2013, doi: 10.1016/j.ajog.2012.10.873.

RUBANA HOQUE CHOWDHURY received the Bachelor of Science (Eng.) degree in electrical and electronic engineering from Chittagong University of Engineering and Technology (CUET), Bangladesh, in 2009, and the Master of Science degree in biomedical engineering from the National University of Malaysia, in 2013. She is currently pursuing the Doctor of Philosophy (Ph.D.) degree in biomedical engineering with Chittagong University of Engineering and Technology.

From 2014 to 2019, she was with Southern University, Bangladesh, as a Lecturer. From 2020 to 2023, she was with Northern University, Bangladesh, as an Assistant Professor. Her contributions to research are evident through his publication of over 16 research papers in international journals and conference proceedings and gathering more than 700 citations on the Scopus database. Her research interests include biosignal processing, artificial intelligence, clinical engineering, algorithm design, and the development and application of machine learning models for the analysis of electrohysterogram data in clinical settings.

QUAZI DELWAR HOSSAIN (Member, IEEE) received the B.Sc. degree in electrical and electronic engineering from Chittagong University of Engineering and Technology (CUET), Chittagong, Bangladesh, in 2001, the Master of Engineering degree in semiconductor electronics and integration sciences from Hiroshima University, Hiroshima, Japan, in 2007, and the Ph.D. degree in microelectronics from the University of Trento, Trento, Italy, in 2010, working on the design and characterization of a current assisted photo mixing demodulator for time-of-flight-based 3-D complementary metal-oxide-semiconductor image sensors. During the Ph.D. degree, he also spent a period with the Smart Optical Sensors and Interfaces Group, Bruno Kessler Foundation, Trento, as a Postgraduate Researcher. From 2001 to 2007, he was with CUET as a Lecturer. In 2007, he became an Assistant Professor with the Faculty of Electrical and Computer Engineering, CUET, where he is currently a Professor. His research interests include CMOS circuit design, simulation and experimental characterization, and biomedical electronics and its applications. He is also a Life Fellow of Institute of Engineers, Bangladesh, and a Life Member of Bangladesh Physical Society.

MOHIUDDIN AHMAD (Member, IEEE) received the B.Sc. (Eng.) degree (Hons.) in electrical and electronic engineering from Chittagong University of Engineering and Technology (CUET), Bangladesh, the M.S. degrees in electronics and information science, specializing in biomedical engineering from Kyoto Institute of Technology, Japan, in 1994 and 2001, respectively, and the Ph.D. degree in computer science and engineering from Korea University, Republic of Korea, in 2008.

In addition, he is the Founder and the President of the ''Clinical Engineering Association—Bangladesh (CEAB),'' a non-political, non-profit organization that aims to enhance patient care through the application of medical equipment. In this role, he oversees the policies and strategic directions of CEAB. He has supervised numerous doctoral and master's theses, focusing on areas such as biomedical signal and image processing, computer vision and pattern recognition, human motion analysis, clinical engineering and modern healthcare, circuits and systems, ICT, artificial intelligence in healthcare, and energy conversion. His contributions to research are evident through his publication of over 180 research papers in international journals and conference proceedings.

Dr. Ahmad holds a Life Fellowship with IEB, membership with IEEE and is a Senior Member of the International Association of Computer Science and Information Technology. In recognition of his academic excellence, he was honored with the Institute Gold Medal by the Prime Minister of Bangladesh. During his career, he has actively participated in various international conferences, serving as the Organizing Chair for EICT 2019; the TPC Chair for EICT 2015; the Co-Chair/Track Chair for events EICT 2013, EICT 2017, EICT 2021, and EICT 2023; and the General Chair for ICICTD 2022 organized by IICT and KUET.